



Responsive Anionophores with AND Logic Multi-Stimuli Activation

Manzoor Ahmad, Toby G. Johnson, Martin Flerin, Fernanda Duarte, and
 Matthew J. Langton*

Abstract: Artificial ion transport systems have emerged as an important class of compounds that promise applications in chemotherapeutics as anticancer agents or to treat channelopathies. Stimulus-responsive systems that offer spatiotemporally controlled activity for targeted applications remain rare. Here we utilize dynamic hydrogen bonding interactions of a 4,6-dihydroxy-isophthalamide core to generate a modular platform enabling access to stimuli-responsive ion transporters that can be activated in response to a wide variety of external stimuli, including light, redox, and enzymes, with excellent OFF-ON activation profiles. Alkylation of the two free hydroxyl groups with stimulus-responsive moieties locks the amide bonds through intramolecular hydrogen bonding and hence makes them unavailable for anion binding and transport. Triggering using a particular stimulus to cleave both cages reverses the hydrogen bonding arrangement, to generate a highly preorganized anion binding cavity for efficient transmembrane transport. Integration of two cages that are responsive to orthogonal stimuli enables multi-stimuli activation, where both stimuli are required to trigger transport in an AND logic process. Importantly, the strategy provides a facile method to post-functionalize the highly active transporter core with a variety of stimulus-responsive moieties for targeted activation with multiple triggers.

Introduction

The transmembrane transport of ions mediated by membrane channels and ion pumps is a fundamental process in biology that controls a wide variety of functions.^[1] These biological transport systems are often gated, whereby the transport activity is controlled in response to the presence of

an external stimulus, such as ligand binding, light, pH, or membrane potential.^[2] Malfunctioning ion channels can trigger life-threatening diseases such as Cystic fibrosis, Bartter syndrome, and Dent's disease.^[3] Artificial supramolecular ion transport systems in the form of ion channels and carriers have emerged as an important class of compounds that not only serve as models to investigate ion transport processes, but also have potential as chemotherapeutics to treat cancer or to replace faulty ion channels.^[4] However, stimulus-responsive ion transport systems that offer spatiotemporally controlled activation for targeted applications are rare.^[5] Stimuli that have been employed for generating responsive behavior include light, pH, redox, ligands, enzymes, and membrane potential.^[6] Reversibly gated systems mostly include the use of photo-switches such as azobenzene,^[7] stiff stilbene^[8] and hydrazones,^[9] where light either controls the ion binding affinities or the self-assembly pattern of the different isomeric forms to control transport activity. Photo-switches have also been used to regulate transport via a relay mechanism^[10] and to control macrocycle shuttling in a membrane-spanning [2] rotaxane transporter.^[11] These systems, however, often exhibit background transport activity in their off state because of incomplete photoconversion, or suffer from fast thermal relaxation which limits their applicability in biological contexts. Irreversible modulation of transport activity, in which activity of a pro-carrier or channel is activated by cleavage of a caging group, provides a route to overcome the challenges of incomplete activation or deactivation in photo-switchable systems, and examples include the use of photocages to either block the anion binding sites,^[12] modulate the self-assembly pattern,^[13] or control the mobility of an anionophore.^[14] Other similar systems include use of redox stimuli to trigger decaging, including for chalcogen bonding anionophores^[15] and Au-(III) caged systems.^[6b] Caging with photo- or redox-labile hydrophilic groups provides a different strategy to inhibit transport, by preventing membrane uptake of the pro-carrier from the aqueous phase, until these groups are removed by a de-caging reaction.^[16] These approaches, whilst enabling effective control over ion transport, require complex design strategies and offer unpredictable outcomes. Methods to access caged anionophores with excellent OFF-ON activation profiles, in which multiple stimulus-responsive moieties can be incorporated in a readily accessible and modular fashion, are lacking. Whilst Liu and co-workers have very recently reported a molecular motor-based logic gate potassium ion channel,^[17] to the best of our knowledge, there are no reported stimulus-responsive ionophores that

[*] Dr. M. Ahmad, Dr. T. G. Johnson, M. Flerin, Prof. F. Duarte, Prof. M. J. Langton
 Chemistry Research Laboratory
 University of Oxford
 Mansfield Road, Oxford, OX1 3TA, UK
 E-mail: matthew.langton@chem.ox.ac.uk

© 2024 The Authors. Angewandte Chemie International Edition published by Wiley-VCH GmbH. This is an open access article under the terms of the Creative Commons Attribution License, which permits use, distribution and reproduction in any medium, provided the original work is properly cited.

require the presence of two stimuli for activation, such as light and cellular redox environment, despite the potential for greatly increased levels of spatiotemporally targeted activation at the intersection of the two stimuli.

Herein, we report a modular platform for responsive anionophores, activatable by a diverse range of stimuli. This enables access to the first example, to the best of our knowledge, of a dual stimuli-triggered AND logic system in which two stimuli are required to trigger ion transport. Based on a core anionophore platform derived from 4,6-dihydroxy-isophthalamide, we demonstrate that double-caging of the hydroxy groups using various protecting groups inhibits transport via the formation of a six-membered intramolecular hydrogen-bonded ring. Decaging of both hydroxy groups reverses the hydrogen bonding pattern, such that the amide N–H protons are available for anion binding and transport. We demonstrated that such a strategy can be employed to incorporate a wide variety of stimulus-responsive cages via post-synthetic modification of the anionophores through the hydroxyl groups, and offers a chemically robust and facile method to generate responsive pro-transporters that respond to multiple stimuli, with excellent OFF-ON activation profiles. We utilize a range of cleavable protecting groups of biological relevance, responding to light and environmental triggers that are overexpressed or generated in cancer tumors, namely an esterase enzyme, H_2O_2 , and H_2S . A mixed stimuli system with AND logic control, requiring the presence of both stimuli for activation, is also accessed from this core scaffold.

Results and Discussion

Design of a Modular, Stimuli-Responsive Transporter Platform

We identified 4,6-dihydroxy-isophthalamide as the key building block for our modular, responsive anionophore platform. This receptor was first reported by Quesada and co-workers in 2007 as a chloride carrier,^[18] and is preorganized via intramolecular hydrogen bonding between the hydroxyl hydrogen bond donors and the adjacent carbonyl groups (Figure 1A). Alkylation of these hydroxy groups disrupts this pattern, leading to an *anti-anti* arrangement of the amides and a decrease in binding affinity. Whilst this project was ongoing, Ren and co-workers reported non-covalently stapled self-assembled H^+/Cl^- channels utilizing a similar approach with alkyl-functionalized dihydroxy isophthalamide derivatives, in which photo-dealkylation of the hydroxyl groups releases the free hydroxyl form to enable H^+/Cl^- transport across the lipid bilayer membrane via a channel mechanism.^[19]

In the present work, we targeted a 4,6-dihydroxy-bis-benzylamide scaffold as the key anionophore core, which we anticipated would be amenable to facile post-synthetic modification with a diverse range of cleavable groups to access the corresponding stimuli-responsive pro-anionophores. We also expected that incorporation of two different stimuli-responsive protecting groups would therefore allow access to an unprecedented AND logic gate, in which the

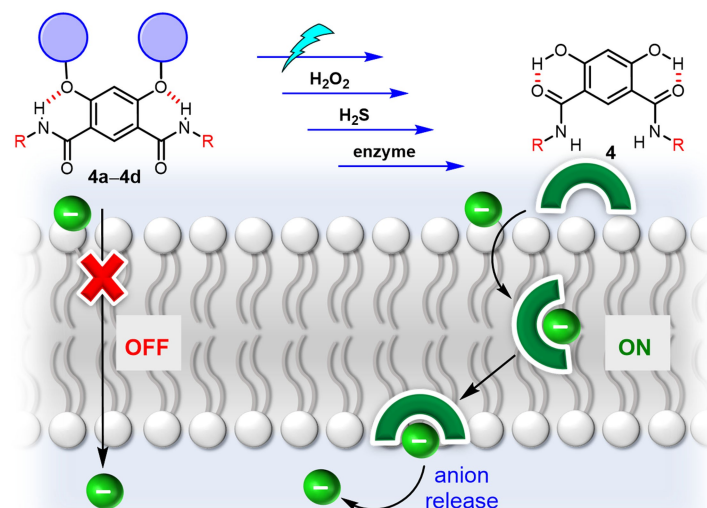
presence of two stimuli is required to activate transport by cleaving both groups. We identified four such protecting groups responding to light, H_2O_2 , esterase, and H_2S , all of biological relevance. Light is a key external stimulus for activation of synthetic or biomolecules, and has shown promises to treat cancer through photodynamic therapy.^[20] Pro-transporters activated by either H_2O_2 or H_2S are of significant interest because elevated concentrations of hydrogen peroxide are a hallmark of tumor microenvironments,^[21] whilst up-regulation of H_2S -producing enzymes is frequently observed in different cancer types.^[22] Similarly, certain esterase enzymes are overexpressed in tumor cells, an observation that has been exploited to target therapeutics,^[23] and therefore enzyme-triggered pro-transporters are of particular interest for potential targeted cancer therapy.

To target these stimuli, we selected suitable protecting groups (cages) that will be cleaved by these stimuli to release the free hydroxyl groups of the 4,6-dihydroxy-isophthalamide anionophore. For photo-activation, we selected the well-established *ortho*-nitrobenzyl (ONB) group, while for H_2O_2 , we identified a cage with boronic ester functionality that in the presence of H_2O_2 undergoes an oxidative conversion to the corresponding phenol, which upon a further intramolecular cascade reaction releases the desired anionophore (Figure 1C).^[24] A methyl pivalate cage was selected for esterase hydrolysis,^[25] and a *para*-azidobenzyl cage for activation with H_2S , which reduces the azide to the corresponding amino derivative,^[26] and through a subsequent intramolecular cascade cleavage releases the anionophore.

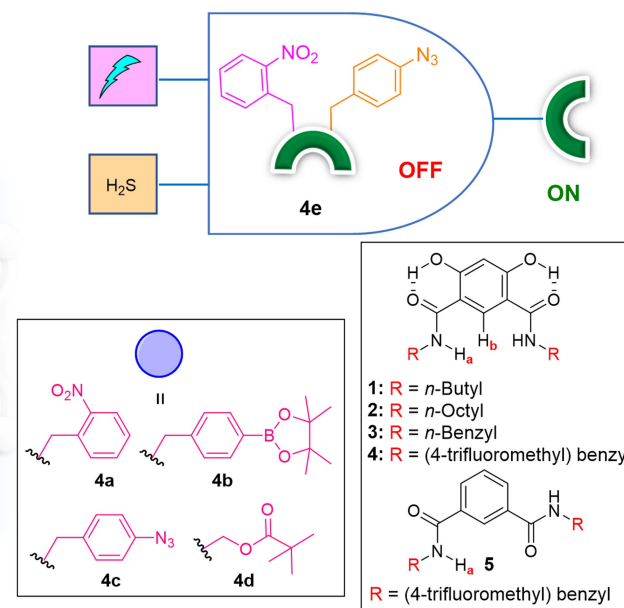
Synthesis and Anion Binding Experiments of Anionophores 1–5

To synthesize the active anionophores **1–4** dibenzylated isophthalic acid **6** was coupled with different aliphatic amines using hexafluorophosphate azabenzotriazole tetramethyl uronium (HATU) as the coupling reagent to yield the dibenzylated amide derivatives **7a–7d**, which upon reaction with hydrogen in the presence of catalytic palladium on charcoal yielded the final active anionophores **1–4** in excellent yields (Figure 2A). Compound **5**, prepared as a control compound lacking the possibility of intra-molecular hydrogen bonding, was synthesized by reacting isophthalic acid **8** with 4-trifluoromethyl benzylamine. To investigate the anion binding capabilities of compounds **1–5**, ^1H NMR titration studies were performed in acetonitrile- d_3 . Addition of increasing equivalents of tetrabutylammonium chloride (TBACl) solution to the receptors **1–5** lead to a significant downfield chemical shift of the amide N–H_a and C_{Ar}–H_b protons respectively (Figure 2C, S43, S45, S47, S49, S51), indicative of N–H_a⋯Cl[−] and C_{Ar}–H_b⋯Cl[−] hydrogen bonding interactions. Analysis of the generated binding isotherms using Bindfit determined 1:1 host:guest association constants ($K_{a(1:1)}/\text{Cl}^-$) of $2,573\text{ M}^{-1} \pm 13\%$ for **1**, $9,423\text{ M}^{-1} \pm 10\%$ for **2**, $20,805\text{ M}^{-1} \pm 12\%$ for **3**, $25,397\text{ M}^{-1} \pm 14\%$ for **4**, and $531\text{ M}^{-1} \pm 4\%$ for **5** respectively (Figure 2D, 2E, S44, S46, S48, S50, S52). The chloride binding affinity sequence

(A) Multi-stimuli responsive caged anionophores



(B) Dual-triggered ion transport with AND logic



(C) Activation mechanisms with light, redox and enzymatic stimuli

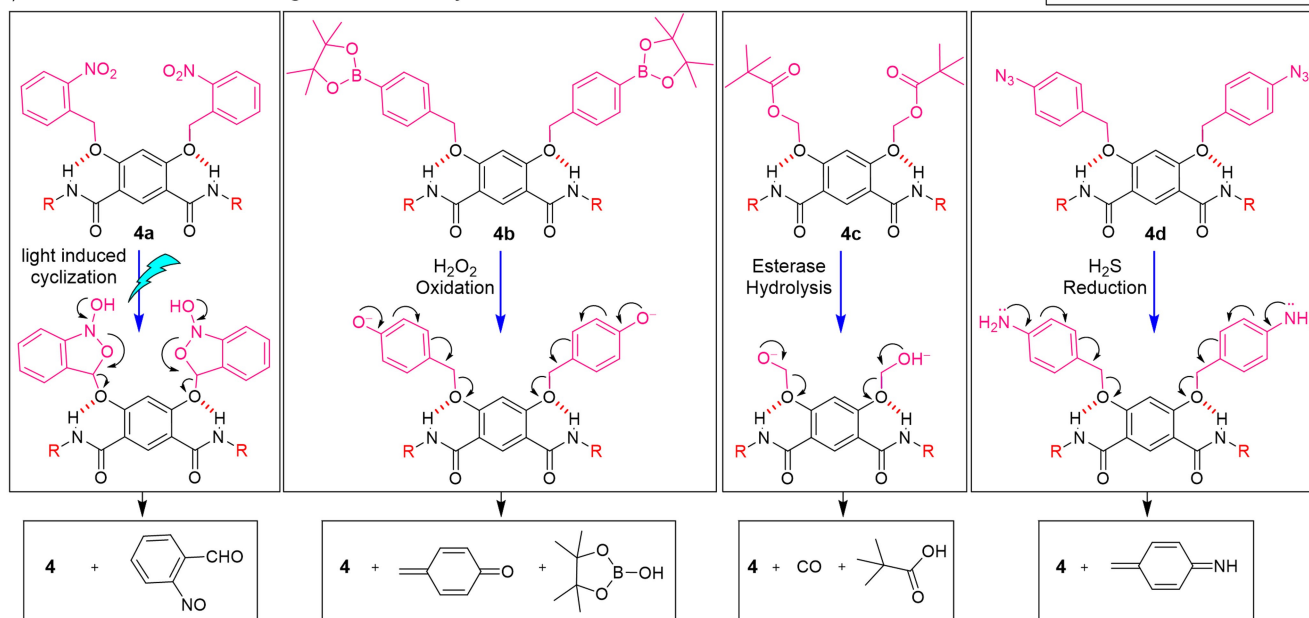


Figure 1. (A). Schematic representation of stimulus responsive ion transport using light, redox, and enzyme. (B) An AND logic dual-triggered anionophore, and chemical structures of active ion transporters 1–5 and stimulus-responsive cage groups. (C) Mechanism of triggered activation of pro-transporters 4a–4d using light, H_2O_2 , H_2S , and enzyme as external stimuli.

was found to be $4 > 3 > 2 > 1 > 5$. Compound 5, which lacks the possibility of intra-molecular hydrogen bonding, displayed much weaker chloride binding compared to compounds 1–4, indicating that the preorganisation of the latter compounds significantly enhances anion affinity. Incorporation of amide linkages with benzyl substituents enhances the chloride binding, presumably due to anion- π interactions as suggested by the upfield shift of benzyl aromatic *meta* protons, and $\text{C}_{\text{Ar}}\text{--H}\cdots\text{Cl}^-$ hydrogen bonding interactions suggested by downfield shift of the benzyl *ortho* protons for the trifluoromethyl benzyl derivative 4 (Figure S49).

Ion Transport Studies

Having determined the chloride binding capabilities of the receptors in solution, ion transport studies for 1–5 were performed using large unilamellar vesicles (LUVs) encapsulating the chloride-sensitive fluorophore lucigenin. LUVs were prepared using 1-palmitoyl-2-oleoyl-sn-glycero-3-phosphocholine (POPC) lipid molecules entrapping 1 mM lucigenin in 200 mM sodium nitrate buffered to pH of 6.5 using 10 mM phosphate buffer. To monitor chloride transport across the LUV membrane, a Cl^- gradient was generated by adding sodium chloride (using 2.0 M NaCl) in the external

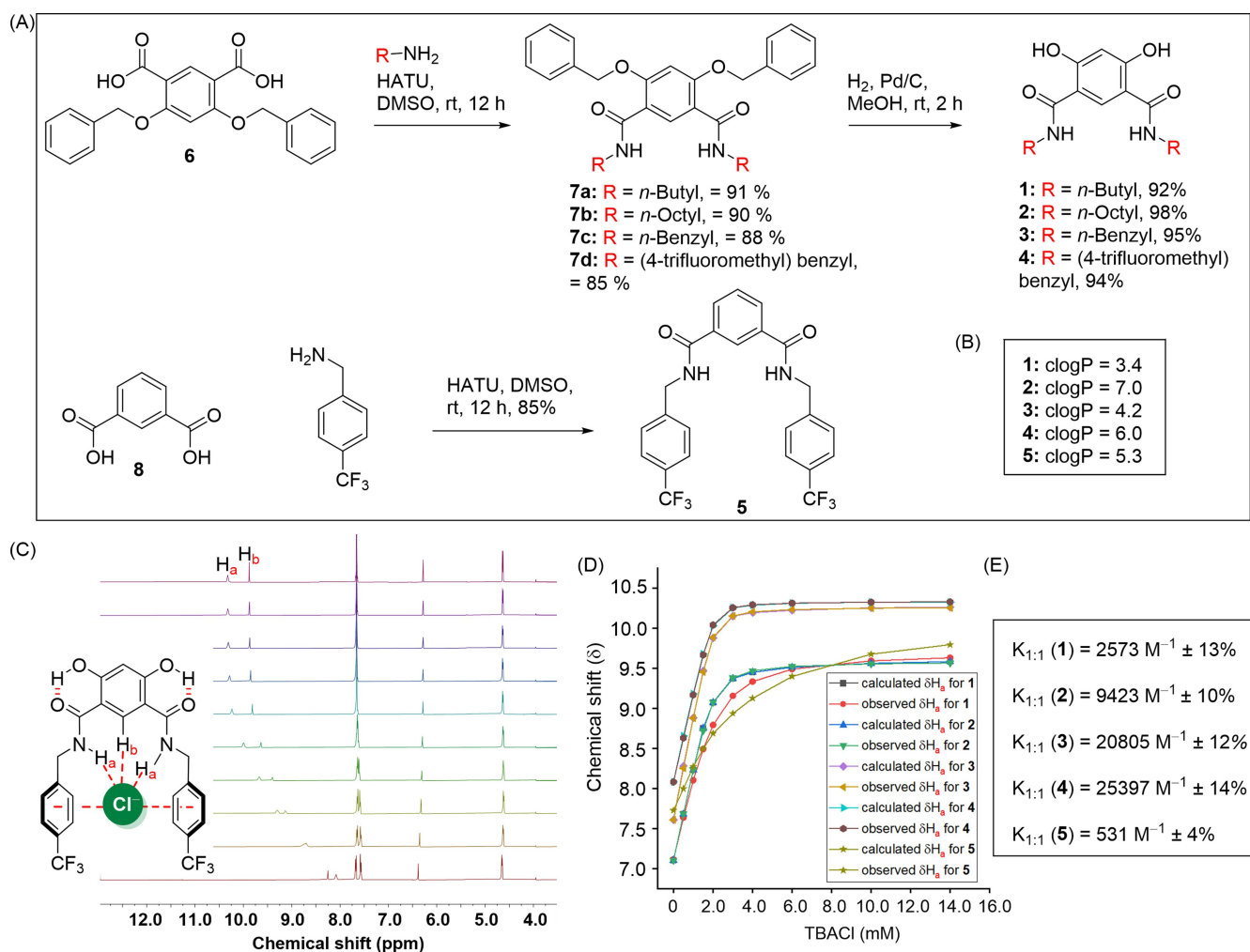


Figure 2. (A) Chemical synthesis of active transporters 1–5. (B) clogP values of transporters 1–5, calculated using MarvinSketch software. (C) Partial ^1H NMR titration of **4** (2.0 mM) with tetrabutylammonium chloride (TBACl, 0–14 mM) in acetonitrile- d_3 . (D) The plot of chemical shift (δ) of H_a proton vs concentration of TBACl added, fitted to 1:1 binding model of BindFit v0.5 for the active transporters 1–5. (E) Binding constant values of transporters 1–5.

buffer to achieve a concentration of 33.3 mM. The anion transport process was monitored by recording the quenching of the lucigenin fluorescence by chloride after the addition of transporters 1–5. Significant quenching was observed for compounds 1–4, whilst a minimal effect was observed for compound 5, suggesting that the intramolecular hydrogen bonding between the hydroxyl protons and the amide carbonyl significantly enhances the ion transport activity, due to the formation of a preorganized binding cavity for anion binding. The ion transport activity sequence of **4** > **3** > **2** > **1** > **5** could therefore be attributed primarily to the sequence of their chloride binding affinities, with minimal impact from the varying lipophilicity of the ionophores (Figure 2B).

Figure 3A shows the effect of the lucigenin fluorescence by the addition of compounds 1–5 (0.608 mol % with respect to lipid). Transporter **4** was found to be the most active, correlating with its enhanced chloride association determined by the ^1H NMR titration studies. We subsequently performed dose-dependent ion transport activity analysis on

the most active transporter **4** (Figure S65A). Hill analysis yielded an EC_{50} value of $0.092 \text{ mol } \% \pm 0.001$. The Hill coefficient (n) was found to be ~ 2 , indicative of the involvement of a 2:1 receptor-anion complex in the transmembrane anion transport process (Figure S65B). This is consistent with results from DFT calculations (see ESI for computational details). These calculations revealed the pre-organization of the binding cavity by intramolecular phenol-carbonyl hydrogen bonding interactions and intermolecular π – π interactions, and the ability of two molecules of **4** to bind to chloride within the transport-active complex via hydrogen bonds (Figure 3F). This 2:1 binding mode is energetically less preferable to 1:1 binding (consistent with results from NMR titration experiments, and a Hill coefficient > 1 in transport experiments which indicates endergonic self-assembly), as a result of elongation of the hydrogen bonding interactions with the chloride anion (Table S1). However, the formation of the 2:1 complex results in much greater encapsulation of the chloride anion, which presumably

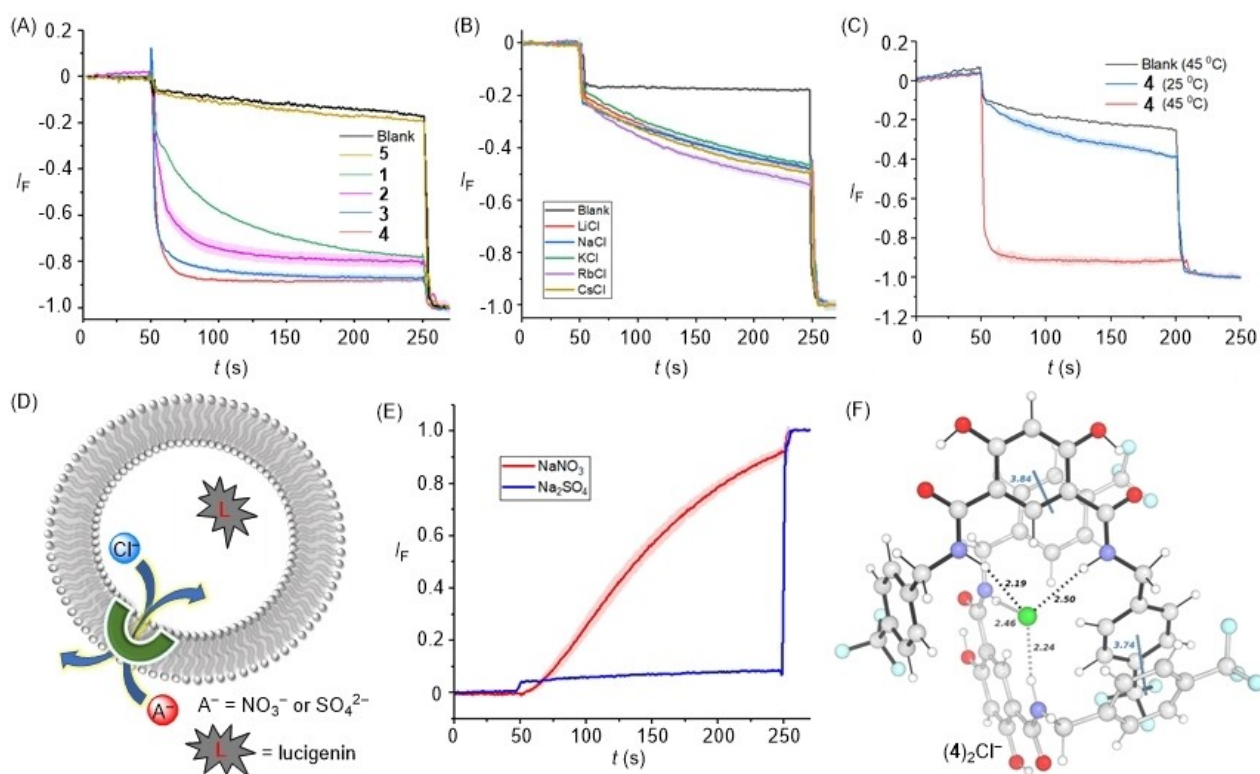


Figure 3. (A) Activity comparison of 1–5 (0.608 mol%) across POPC-LUVs/lucigenin. (B) Cation selectivity of 4 (0.152 mol%) by varying the external cations using different MCl external buffers ($\text{M}^+ = \text{Li}^+, \text{Na}^+, \text{K}^+, \text{Rb}^+, \text{Cs}^+$). (C) Ion transport activity of 4 (0.608 mol%) across DPPC-based vesicles at 25 °C and 45 °C temperatures, respectively. (D) Schematic representation of lucigenin-based chloride efflux using either extravesicular SO_4^{2-} or NO_3^- ions. (E) Ion transport activity of 4 (0.608 mol%) in presence of external SO_4^{2-} and NO_3^- ions. (F) The geometry-optimized structure of $[(4)_2\text{Cl}^-]$ complex, optimised at the $\omega\text{B97X-D3/def2-SVP}$ level of theory.

lowers the barrier for membrane translocation such that the 2:1 complex is the dominant transport-active species.

Variation of the cation in the external buffer using different MCl solutions ($\text{M}^+ = \text{Li}^+, \text{Na}^+, \text{K}^+, \text{Rb}^+, \text{Cs}^+$) did not affect the ion transport activity, ruling out the possible M^+/Cl^- symport pathway for chloride transport (Figure 3B). To distinguish between the possible $\text{Cl}^-/\text{NO}_3^-$ antiport and H^+/Cl^- symport pathways, we performed a modified lucigenin-based transport assay in which LUVs encapsulating lucigenin and NaCl were suspended in a buffered solution of either Na_2SO_4 or NaNO_3 . Appreciable transport with 4 was observed only in the case of external nitrate (Figure 3E). This suggests that $\text{Cl}^-/\text{NO}_3^-$ antiport pathway is the dominant mechanism, rather than H^+/Cl^- symport for which no difference in the transport rate would be observed by changing the salts in the external buffer. In the case of the Cl^-/X^- antiport mechanism, transport of either NO_3^- or SO_4^{2-} is required to drive the efflux of chloride ions, the latter being too hydrophilic to be readily transported. Evidence for a mobile carrier mechanism of transport was obtained by conducting analogous experiments in dipalmitoylphosphatidylcholine (DPPC) LUVs. Suppressed activity at 25 °C, and increased activity at 45 °C which is above the gel–liquid phase transition temperature for DPPC lipid ($T_m = 41$ °C), is indicative of a mobile carrier process, rather than a self-assembled ion channel pathway, the activity of

which would be typically expected to be invariant to lipid phase (Figure 3C).

Synthesis and Anion Binding Experiments of Caged Pro-Transporters 4a–4d

Compound 4, with the optimum anion binding and transport capabilities, was selected for caging with different stimulus-responsive protecting groups. Alkylation of 4 with 1-(bromomethyl)-2-nitrobenzene, 4-bromomethylphenylboronic acid, or 1-azido-4-(bromomethyl)benzene gave the corresponding light, H_2O_2 or H_2S responsive anionophores 4a, 4b and 4c respectively (Figure 4A). Reaction of 4 with iodomethyl pivalate 9d furnished the corresponding esterase responsive anionophore 4d. ^1H NMR chloride binding experiments were performed with 4a–4d to explore the effect of intramolecular hydrogen bonding of the amide protons on the chloride binding process, by the addition of increasing equivalents of TBACl to the caged compounds 4a–4d in acetonitrile- d_3 . No change in the chemical shift for the amide protons was observed for these four caged compounds, which demonstrates the lack of chloride binding (Figure 4C, S53–S56) and confirms that the intramolecular hydrogen bonding of the amide NH groups renders them unavailable for anion recognition.

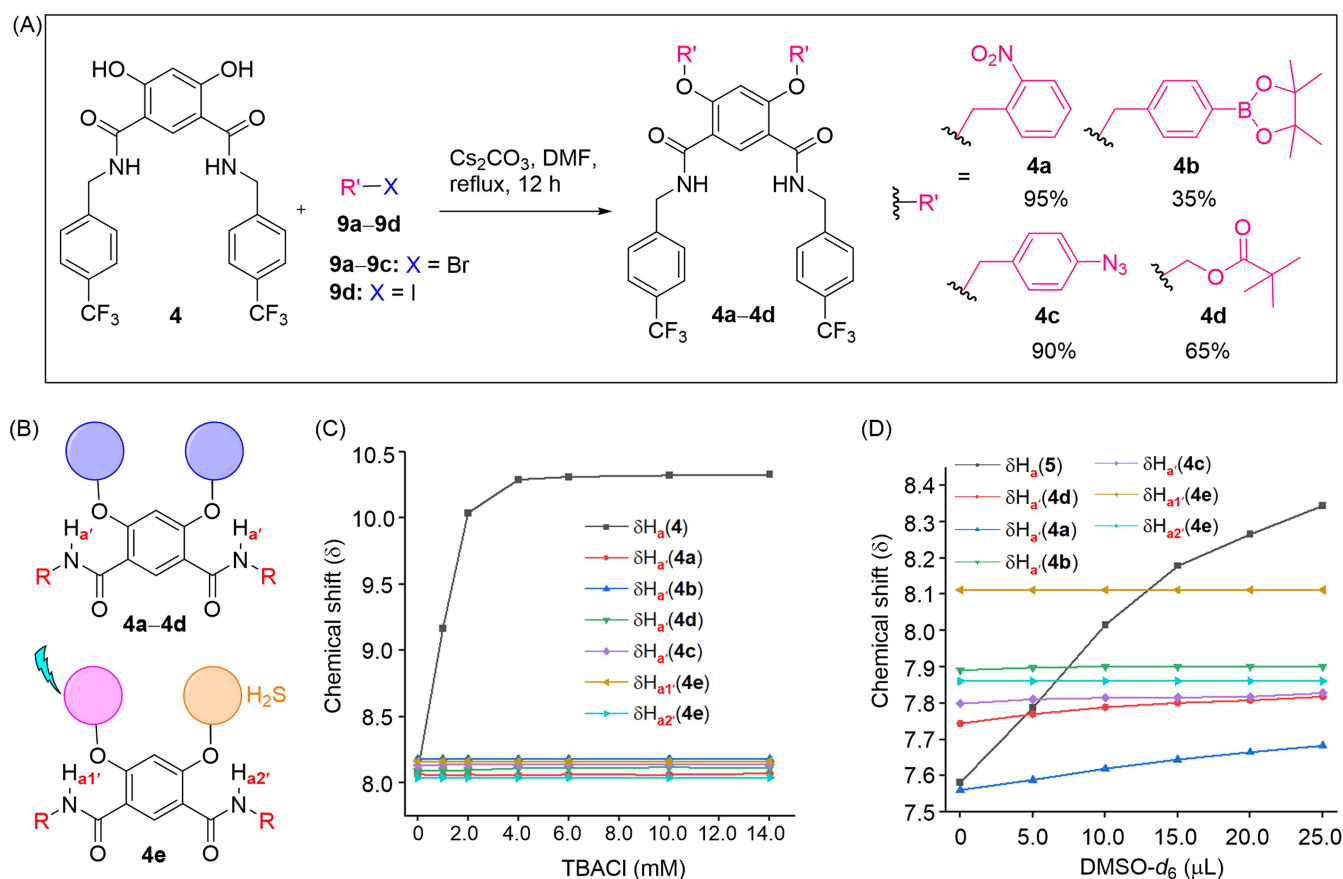


Figure 4. (A) Chemical synthesis of caged pro-transporters **4a–4d**. (B) Chemical structures of **4a–4e** showing H_a and $H_{a'}$ protons. (C) Change in chemical shift values of H_a or $H_{a'}$ upon titrating **4**, **4a–4e** with tetrabutylammonium chloride in acetonitrile- d_3 . (D) Change in chemical shift values of H_a (compounds **4,5**) or $H_{a'}$ (compounds **4a–4e**) upon titrating with DMSO- d_6 in $CDCl_3$.

Furthermore, negligible changes to the spectra upon the addition of DMSO- d_6 to the caged samples in chloroform- d_3 also confirms that the amide protons are engaged in intramolecular hydrogen bonding, and unable to interact with the DMSO hydrogen bond acceptor (Figure 4D, S58–S62). In contrast, the amide proton of control compound **5**, which does not have the possibility of intramolecular hydrogen bonding, showed a significant downfield chemical shift upon the addition of DMSO.

Stimuli-Responsive Ion Transport Activation

Stimuli-responsive activation studies on pro-transporters **4a–4d** were initially performed in solution phase experiments. For **4a** and **4b**, a solution of the pro-transporter in DMSO- d_6 was subjected to the relevant stimulus: a 405 nm LED (1 W) for **4a**, and incubation of **4b** with H_2O_2 (50 eq.) at 37 °C (Figure S68, S69). For **4c**, a solution of the pro-transporter in a mixture of methanol- d_4 :acetone- d_6 (4:1) was subjected to sodium hydrosulfide ($NaSH$, 20 eq.) as the H_2S donor (Figure S70). For **4d**, the pro-transporter was incubated with porcine liver esterase in a THF/DMSO/ H_2O (1:1:1) mixture at 37 °C. 1H NMR and UV/Vis analysis were used to monitor the decaging reactions of **4a–4c** over time,

while HPLC was employed for the enzyme-activated **4d** (Figure S71, see the ESI for full experimental details).

In each case, efficient decaging to generate **4** was observed (>85 % conversion). With evidence of efficient activation of pro-transporters **4a–4d** using light, H_2O_2 , esterase, and H_2S in the solution phase in hand, the triggered OFF-ON activation of ion transport was subsequently evaluated using lucigenin-containing LUVs in buffered $NaNO_3$ solution. Pro-transporters **4a**, **4b**, **4c**, or **4d** were added in an aliquot of DMF (final concentration of 0.608 mol % with respect to lipid), followed by an external chloride pulse. No significant changes were observed in the lucigenin fluorescence, indicating that the pro-transporters are inactive at this concentration, thus achieving an effective OFF state.

We then subjected samples of the pro-transporters **4a–4d** in buffer solution in a cuvette to the various stimuli, before adding LUVs and performing ion transport experiments by addition of a chloride pulse. Figure 5 shows the activation of chloride transport by stimulus-triggered decaging of the pro-transporters (0.66 μM , 0.608 mol %) after subjecting the samples to the stimulus for various time intervals. Photo-activation of **4a** using a 1 W 405 nm LED resulted in efficient activation, achieving comparable activity to a sample of **4** after 120 s of irradiation, indicative of near

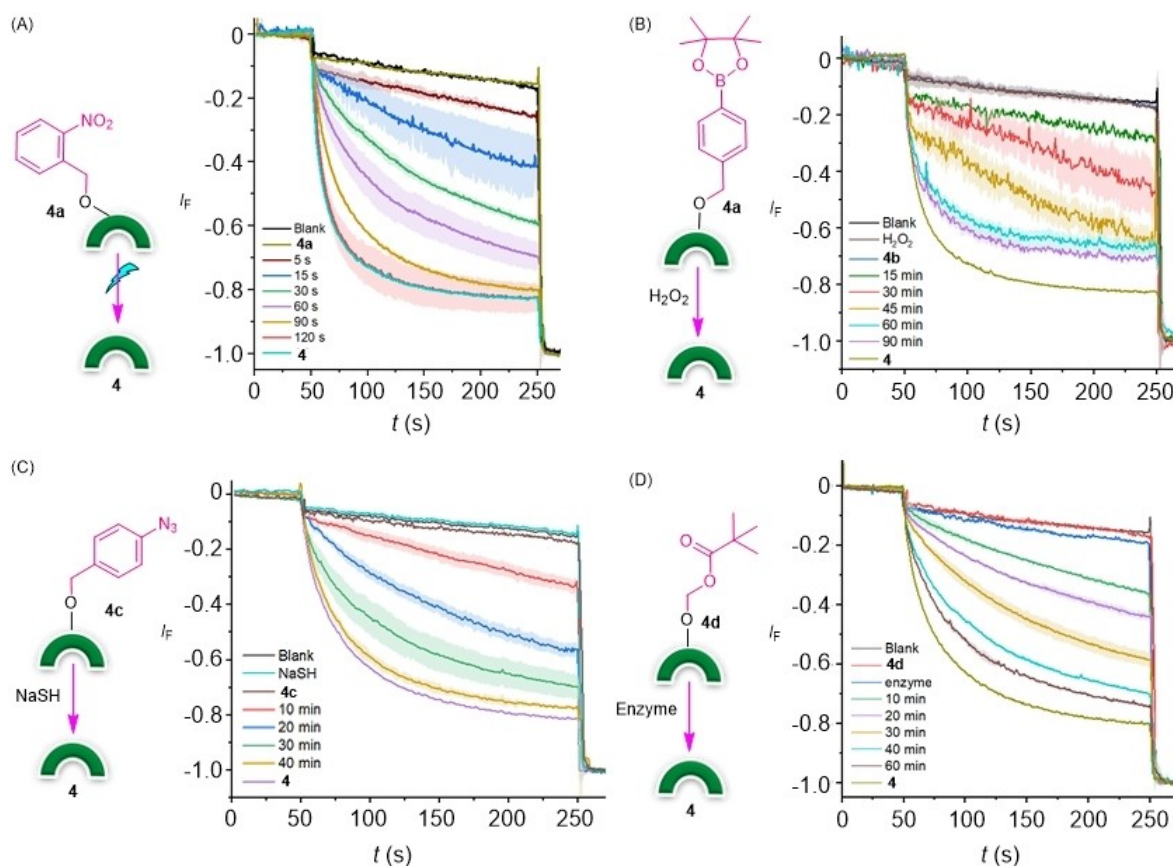


Figure 5. (A) Ion transport activities across POPC-LUVs containing lucigenin, by photo-irradiating **4a** at 405 nm light using an LED (1 W); (B) by treating **4b** with H_2O_2 (50 eq.); (C) by reacting **4c** with NaSH (10 eq.) and (D) by treating **4d** with porcine liver esterase enzyme.

quantitative decaging under these conditions (Figure 5A). Effective activation of the boronic-acid pro-transporter **4b** in the presence of 50 eq. H_2O_2 was also achieved, with approximately 86 % activation of ion transport observed after incubation at 37°C for ~90 minutes (compared to a sample of **4**, assuming transport activity as 100 % immediately prior to LUV lysis). As expected, the extent of ion transport activation with time was dependent on peroxide concentration (Figure S77). Control experiments in the absence of **4b** demonstrated that the LUVs are stable to peroxide after incubation for 2 hours (brown data, Figure 5B), while **4b** remained inactive to transport after incubation in buffer for 2 hours, indicating that the cage is stable in the absence of peroxide (blue data). Similarly, **4c** was activated in the presence of 10 eq. NaSH, generating transport activity ~93 % that of as-synthesized **4** (Figure 5C). Analogous control experiments to those conducted with **4b** revealed that the cage is stable in the absence of the stimulus (brown data); that the LUVs are stable to NaSH (cyan data); and that the extent of activation is dependent on NaSH concentration (Figure S78). Finally, activation of **4d** using an esterase was achieved by incubating the pro-transporter with 0.034 mg/mL porcine liver esterase at 37°C for various time intervals, before conducting the anion transport experiments (Figure 5D). Up to 89 % activation could be achieved compared to **4**, with the activation again

strongly dependent on concentration (Figure S79). No change in transport activity was observed with only **4d** in the absence of enzyme for 1 hour, indicating that the enzyme does not affect vesicle integrity and that pro-transporter **4d** is itself stable in solution.

AND Logic Activation Using a Dual-Caged Transporter

Given the facile functionalization of **4** with various stimuli-responsive protecting groups, we sought to access a dual-stimuli-responsive system, in which two protecting groups triggered by orthogonal stimuli are incorporated to access an AND logic gate, i.e., both stimuli are required to release the transporter. Accordingly, we prepared a dual light/ H_2S triggered AND logic transporter **4e** to exemplify this concept by successive alkylation of **4** with the appropriate bromo-benzyl derivatives (Figure 6A, see ESI for further details). ^1H NMR experiments confirmed that, as with the bis-caged derivatives **4a–4d**, the presence of the two different protecting groups inhibited anion binding (Figure S57). Similarly, no chemical shift changes were observed upon titrating **4e** with DMSO- d_6 in CDCl_3 (Figure S63).

We initially examined the activation of **4e** in the solution phase by irradiating with 405 nm light followed by the addition of 10 eq. NaSH (Figure S72), or in the opposite

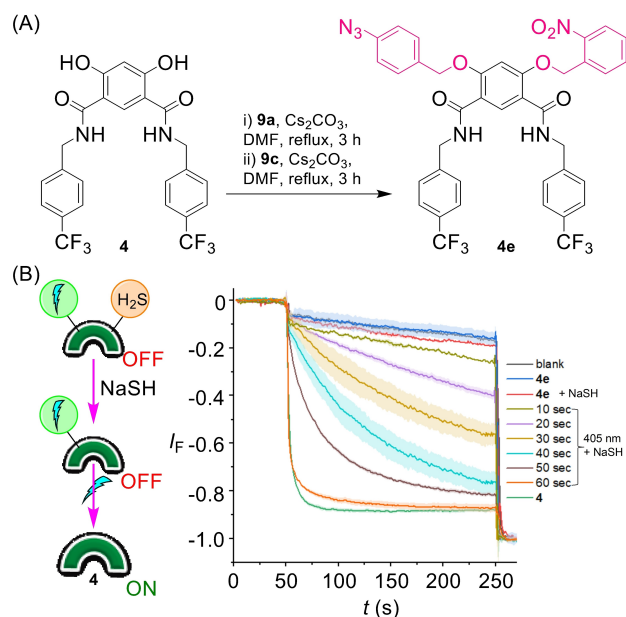


Figure 6. AND logic dual stimuli-responsive anionophore. (A) Synthesis of **4e**. (B) Transport activity of **4e** in response to treating with NaSH (5.0 eq, as D₂O solution (0.5 M)) followed by photoirradiation at 405 nm (1 W LED).

order (Figure S73). In both experiments, significant activation of **4e** was achieved, generating the corresponding free transporter **4**. We subsequently examined the AND logic activation of ion transport, by conducting similar anion transport experiments to those described previously. Irradiation of **4e** with 405 nm light to cleave the photocage (Figure S80), or incubation of **4e** with NaSH (Figure 6B, red data), did not lead to transport activation, demonstrating the requirement for both cages to be cleaved in order to generate the required hydrogen bonding arrangement for anion binding and transport. However, following both photo-irradiation and incubation with NaSH, efficient activation of transport was observed, comparable to that of a pristine sample of **4** (Figure 6B). Moreover, the activation could be achieved by applying the stimuli in either order: either by photo-irradiating **4e** initially with 405 nm of light followed by addition of NaSH (5.0 eq) (Figure S80) or by treating **4e** initially with NaSH followed by photoirradiation at 405 nm (Figure 6B). To the best of our knowledge, this represents the first example of an AND logic gate responsive ionophore, requiring the presence of two stimuli for activation, notably achieved with an excellent OFF-ON activation profile.

Conclusion

In conclusion, we have developed a modular platform for accessing stimuli-responsive anionophores, including those requiring multiple stimuli for activation, via post-synthetic modification of a dynamic hydrogen bonding anionophore. By exploiting a 4,6-dihydroxy-isophthalamide scaffold, we demonstrated that alkylation of the hydroxy groups with

various stimulus-responsive caging groups inhibits transport by locking the amide protons into intra-molecular hydrogen bonding interactions, thus preventing chloride binding. Activation using a range of biologically relevant stimuli including light, peroxide, sulfide, and an esterase cleaves the corresponding cage, reversing the intramolecular hydrogen bonding pattern to enable chloride binding and transport. By incorporating two different stimuli-responsive cages, we developed an AND logic gate, in which OFF-ON transport activation is achieved only in the presence of both stimuli. The approach we report here allows for facile access to a range of stimuli-responsive transporters by simple post-synthetic modification of the anionophore, unlike existing approaches which typically require complex, de-novo design strategies to incorporate the desired stimuli-responsive behavior. We anticipate that this AND logic approach in which the presence of two stimuli is required for transporter activation, could be exploited for developing future targeted therapeutics, triggered, for example, by both the local tumor environment (enzymes, redox) and further targeted by an external stimulus such as light.

Acknowledgements

M.A. and M.J.L. acknowledge the Leverhulme Trust (RPG-2020-130) for financial support. T.G.J. thanks the Royal Society and Exeter College, Oxford for funding. M.F. thanks the Centre for Doctoral Training in Synthesis for Biology and Medicine for a studentship, generously supported by GlaxoSmithKline, MSD, Syngenta and Vertex. M.J.L. is a Royal Society University Research Fellow.

Conflict of Interest

The authors declare no conflict of interest.

Data Availability Statement

The data that support the findings of this study are available in the supplementary material of this article.

Keywords: anion transport • stimuli-responsive • membranes • hydrogen bonding • anions

- [1] a) W. D. C. Stein, *Carriers, and Pumps: An Introduction to Membrane Transport*, Academic Press: San Diego, CA **1990**; b) S. B. H. Hladky, D. A. Ion, *Movement in Gramicidin Channels. In Current Topics in Membranes and Transport*, F. Bronner, Ed.; Academic Press: New York **1984**, Vol. 21, pp 327–372; c) B. Hille, *Ion Channels of Excitable Membranes*, 3rd Edition **2001**, Sinauer.
- [2] a) G. Nagel, D. Ollig, M. Fuhrmann, S. Kateriya, A. M. Musti, E. Bamberg, P. Hegemann, *Science* **2002**, 296, 2395; b) W. A. Catterall, *Annu. Rev. Biochem.* **1995**, 64, 493–531; c) M. Jaiteh, A. Taly, J. Hénin, *PLoS One* **2016**, 11, e0151934.

- [3] a) R. D. Vaughan-Jones, K. W. Spitzer, P. Swietach, *J. Mol. Cell. Cardiol.* **2009**, *46*, 318–331; b) T. J. Jentsch, C. A. Hübner, J. C. Fuhrmann, *Nat. Cell Biol.* **2004**, *6*, 1039–1047; c) J. Y. Choi, D. Muallem, K. Kiselyov, M. G. Lee, P. J. Thomas, S. Muallem, *Nature* **2001**, *410*, 94–97.
- [4] a) J. T. Davis, P. A. Gale, R. Quesada, *Chem. Soc. Rev.* **2020**, *49*, 6056–6086; b) A. P. Davis, D. N. Sheppard, B. D. Smith, *Chem. Soc. Rev.* **2007**, *36*, 348–357; c) J. T. Davis, O. Okunola, R. Quesada, *Chem. Soc. Rev.* **2010**, *39*, 3843–3862; d) S. Matile, A. Vargas Jentzsch, J. Montenegro, A. Fin, *Chem. Soc. Rev.* **2011**, *40*, 2453–2474; e) N. Busschaert, C. Caltagirone, W. Van Rossom, P. A. Gale, *Chem. Rev.* **2015**, *115*, 8038–8155; f) P. A. Gale, J. T. Davis, R. Quesada, *Chem. Soc. Rev.* **2017**, *46*, 2497–2519; g) L. E. Bickerton, T. G. Johnson, A. Kerckhoffs, M. J. Langton, *Chem. Sci.* **2021**, *12*, 11252–11274.
- [5] a) M. J. Langton, *Nat. Chem. Rev.* **2021**, *5*, 46–61; b) M. Ahmad, S. A. Gartland, M. J. Langton, *Angew. Chem. Int. Ed.* **2023**, *62*, e202308842; c) J. de Jong, J. E. Bos, S. J. Wezenberg, *Chem. Rev.* **2023**, *123*, 8530–8574.
- [6] a) E. N. W. Howe, N. Busschaert, X. Wu, S. N. Berry, J. Ho, M. E. Light, D. D. Czech, H. A. Klein, J. A. Kitchen, P. A. Gale, *J. Am. Chem. Soc.* **2016**, *138*, 8301–8308; b) A. Roy, O. Biswas, P. Talukdar, *Chem. Commun.* **2017**, *53*, 3122–3125; c) Y. R. Choi, G. C. Kim, H.-G. Jeon, J. Park, W. Namkung, K.-S. Jeong, *Chem. Commun.* **2014**, *50*, 15305–15308; d) E. B. Park, K.-S. Jeong, *Chem. Commun.* **2015**, *51*, 9197–9200; e) M. M. Tedesco, B. Ghebremariam, N. Sakai, S. Matile, *Angew. Chem. Int. Ed.* **1999**, *38*, 540–543; f) G. A. Woolley, M. K. Kapral, C. M. Deber, *FEBS Lett.* **1987**, *224*, 337–342; g) N. Akhtar, N. Pradhan, A. Saha, V. Kumar, O. Biswas, S. Dey, M. Shah, S. Kumar, D. Manna, *Chem. Commun.* **2019**, *55*, 8482–8485; h) M. Fares, X. Wu, D. Ramesh, W. Lewis, P. A. Keller, E. N. W. Howe, R. Pérez-Tomás, P. A. Gale, *Angew. Chem. Int. Ed.* **2020**, *59*, 17614–17621; i) A. Docker, T. G. Johnson, H. Kuhn, Z. Zhang, M. J. Langton, *J. Am. Chem. Soc.* **2023**, *145*, 2661–2668; j) X. Wu, J. R. Small, A. Cataldo, A. M. Withecombe, P. Turner, P. A. Gale, *Angew. Chem. Int. Ed.* **2019**, *58*, 15142–15147.
- [7] a) M. Ahmad, S. Metya, A. Das, P. Talukdar, *Chem. Eur. J.* **2020**, *26*, 8703–8708; b) A. Kerckhoffs, Z. Bo, S. E. Penty, F. Duarte, M. J. Langton, *Org. Biomol. Chem.* **2021**, *19*, 9058–9067; c) A. Kerckhoffs, M. J. Langton, *Chem. Sci.* **2020**, *11*, 6325–6331.
- [8] S. J. Wezenberg, L.-J. Chen, J. E. Bos, B. L. Feringa, E. N. W. Howe, X. Wu, M. A. Siegler, P. A. Gale, *J. Am. Chem. Soc.* **2022**, *144*, 331–338.
- [9] a) M. Ahmad, D. Mondal, N. J. Roy, T. Vijayakanth, P. Talukdar, *ChemPhotoChem* **2022**, *n/a*, e202200002; b) M. Ahmad, S. Chattopadhyay, D. Mondal, T. Vijayakanth, P. Talukdar, *Org. Lett.* **2021**, *23*, 7319–7324.
- [10] T. G. Johnson, A. Sadeghi-Kelishadi, M. J. Langton, *J. Am. Chem. Soc.* **2022**, *144*, 10455–10461.
- [11] C. Wang, S. Wang, H. Yang, Y. Xiang, X. Wang, C. Bao, L. Zhu, H. Tian, D.-H. Qu, *Angew. Chem. Int. Ed.* **2021**, *60*, 14836–14840.
- [12] a) M. Ahmad, N. J. Roy, A. Singh, D. Mondal, A. Mondal, T. Vijayakanth, M. Lahiri, P. Talukdar, *Chem. Sci.* **2023**, *14*, 8897–8904; b) S. B. Salunke, J. A. Malla, P. Talukdar, *Angew. Chem. Int. Ed.* **2019**, *58*, 5354–5358.
- [13] C. Bao, M. Ma, F. Meng, Q. Lin, L. Zhu, *New J. Chem.* **2015**, *39*, 6297–6302.
- [14] L. E. Bickerton, M. J. Langton, *Chem. Sci.* **2022**, *13*, 9531–9536.
- [15] a) G. Park, F. P. Gabbai, *Chem. Sci.* **2020**, *11*, 10107–10112; b) B. Zhou, F. P. Gabbai, *Chem. Sci.* **2020**, *11*, 7495–7500.
- [16] Y. R. Choi, B. Lee, J. Park, W. Namkung, K.-S. Jeong, *J. Am. Chem. Soc.* **2016**, *138*, 15319–15322.
- [17] C. Li, Y. Wu, Y. Zhu, J. Yan, S. Liu, J. Xu, S. Fa, T. Yan, D. Zhu, Y. Yan, J. Liu, *Adv. Mater.* **2024**, 2312352.
- [18] P. V. Santacroce, J. T. Davis, M. E. Light, P. A. Gale, J. C. Iglesias-Sánchez, P. Prados, R. Quesada, *J. Am. Chem. Soc.* **2007**, *129*, 1886–1887.
- [19] Q. Zhong, Y. Cao, X. Xie, Y. Wu, Z. Chen, Q. Zhang, C. Jia, Z. Wu, P. Xin, X. Yan, Z. Zeng, C. Ren, *Angew. Chem. Int. Ed.* **2024**, *63*, e202314666.
- [20] D. E. J. G. J. Dolmans, D. Fukumura, R. K. Jain, *Nat. Rev. Cancer* **2003**, *3*, 380–387.
- [21] M. López-Lázaro, *Cancer Lett.* **2007**, *252*, 1–8.
- [22] a) C. Szabo, C. Coletta, C. Chao, K. Módos, B. Szczesny, A. Papapetropoulos, M. R. Hellmich, *Proc. Natl. Acad. Sci. USA* **2013**, *110*, 12474–12479; b) *Chemistry, Biochemistry and Pharmacology of Hydrogen Sulfide* (Eds. P. K. Moore, M. Whiteman), Springer International Publishing Switzerland **2015**.
- [23] H. Dong, L. Pang, H. Cong, Y. Shen, B. Yu, *Drug Delivery* **2019**, *26*, 416–432.
- [24] P. Chauhan, S. Jos, H. Chakrapani, *Org. Lett.* **2018**, *20*, 3766–3770.
- [25] P. Chauhan, P. Bora, G. Ravikumar, S. Jos, H. Chakrapani, *Org. Lett.* **2017**, *19*, 62–65.
- [26] H. Chen, X. He, M. Su, W. Zhai, H. Zhang, C. Li, *J. Am. Chem. Soc.* **2017**, *139*, 10157–10163.

Manuscript received: February 16, 2024

Accepted manuscript online: March 22, 2024

Version of record online: April 11, 2024